International Information and Engineering Technology Association
Advancing the World of Information and Engineering

Journal Européen des Systèmes Automatisés
Vol. 59, No. 6, June, 2026, pp. 1631-1639
Journal homepage: http://iieta.org/journals/jesa

Performance Investigation of RIS-Enabled MU-MISO ISAC Systems: A WMMSE-Based Optimization Framework

Huda Mohammed Noori[1*], Abdulrahman Kh. Alhafid[2]

[1] Electrical Engineering Department, College of Engineering, University of Mosul, Mosul 41002, Iraq
[2] Department of Communications and Intelligent Digital Systems Engineering, College of Engineering, University of Mosul, Mosul 41002, Iraq

Corresponding Author Email: abdulrhman.alhafid@uomosul.edu.iq

https://doi.org/10.18280/jesa.590610

Received: 13 April 2026
Revised: 5 June 2026
Accepted: 17 June 2026
Available online: 30 June 2026

Keywords:
integrated sensing and communication, reconfigurable intelligent surface, weighted minimum mean square error, manifold optimization

ABSTRACT

The concept of integrated sensing and communication (ISAC) has recently become a pivotal paradigm for future wireless communication systems. In this technology, the resources of spectrum and hardware are used in a shared manner for both communication and sensing operations. In this context, reconfigurable intelligent surfaces (RISs) have attracted significant interest due to their capability to intelligently control wireless propagation environments, particularly in millimeter-wave (mmWave) systems. In this work, the performance of an RIS-aided ISAC scheme is investigated. While, multiple-input single-output (MISO) downlink network with multiple users is considered. The multi-antenna base station (BS), with the assistance of an RIS, serves multiple user equipment (UEs), each with a single antenna, while simultaneously performing sensing operations. To improve the performance of the ISAC system, a unified optimization framework is developed for optimizing the BS transmit beamforming and RIS reflection coefficients, subject to some operational constraints of the BS and RIS. The formulated non-convex optimization problem is addressed using weighted minimum mean square error (WMMSE) optimization for the beamforming at the BS, while the RIS phase shift profile is optimized through manifold optimization with the constraint of unit modulus. Numerical evaluations demonstrate that the proposed RIS-aided ISAC scheme provides noticeable gains over both the conventional system without RIS and random RIS deployment. The performance of the proposed model indicates notable enhancements in achievable sum-rate and sensing sum signal-to-noise ratio (sum-SNR), while a reduction in outage probability is achieved. The obtained results also highlight the inherent trade-off between communication efficiency and sensing performance in integrated ISAC networks.

1. INTRODUCTION

Wireless communication systems have advanced rapidly to accommodate the stringent requirements of beyond 5G and 6G networks. Recently, integrated sensing-and-communications (ISAC) attracted considerable attention as a new paradigm that integrates wireless communication and sensing within a shared spectrum and resource availability. Unlike conventional systems, where communication and sensing are treated as independent functionalities, ISAC exploits the common physical properties of electromagnetic signals to enable simultaneous data transmission and sensing. This integration improves overall resource utilization efficiency. ISAC has proven to be an important enabler of future intelligent applications such as intelligent vehicles, unmanned aerial vehicles (UAVs), smart cities, and intelligent industrial systems. The general aim of this is to improve the accuracy of sensing with high communication performance. ISAC has also gained much attention from international standardization organizations such as 3GPP, IEEE, and ITU, which identify ISAC as a promising candidate technology for 6G wireless communication [1, 2].

To further improve the performance of ISAC, reconfigurable intelligent surfaces (RIS) are proposed as a prospective candidate. The intelligent control of the wireless propagation environment by means of an RIS can be utilized to direct the signal towards the intended user to improve the received signal quality and reduce interference and fading effects [3-5]. Due to the hardware simplicity, energy efficiency, and cost-effectiveness of the RIS concept, it is widely viewed as a promising candidate to facilitate ISAC in the context of 5G/6G wireless systems. Traditionally, ISAC systems have been characterized by two paradigms: radar communication coexistence (RCC) and dual-functional radar communication (DFRC). In RCC-based ISAC systems, radar communication and communication tasks are carried out independently using separate signals in such a way that interference is minimized. In DFRC-based ISAC systems, radar communication and communication tasks are carried out simultaneously using a single waveform and transmitter. In practical ISAC systems, communication and sensing use the same wireless resources, which may cause interference and affect the overall system performance. RIS can help improve the wireless channel and enhance both communication and sensing performance by adjusting the reflected signals [6, 7]. Initial studies of ISAC system design have been centered on single-cell systems. Then, these systems have been expanded to multi-cell systems, where cooperation among base stations (BS) has been utilized to improve the coverage of the system, the accuracy of the sensing, and to reduce the inter-cell interference. In addition, the ISAC system has moved away from traditional sensing towards multimodal sensing systems, where edge intelligence has been incorporated to allow for efficient data management, as required by next-generation system applications [8-10].

Several research studies have investigated the potential of integrating RIS with ISAC systems to improve communication as well as sensing. In these research studies, the primary aim of the optimization was to enhance the overall sum rate for communication users while maintaining satisfactory high sensing performance. Motivated by these advancements, Luo et al. [11] investigated an RIS-based ISAC system where the beamforming and RIS optimization are employed to maximize the weighted radar sum signal-to-noise ratio (sum-SNR) for the purpose of target detection, under communication quality of service (QoS) and power constraints. An efficient optimization strategy is employed by integrating majorization-minimization, penalty-based, and manifold optimization techniques to achieve notable performance gains. Samir et al. [12] investigate an RIS-assisted ISAC system designed to enhance both communication and sensing performance. The authors aimed to improve the sum-rate while maintaining a required sensing quality measured by the SCNR metric. To address the associated non-convex optimization challenge, manifold optimization techniques were employed for the joint optimization of the transmit beamforming and RIS phase shifts. The proposed method was developed for multiple-user and multiple sensing targets scenarios in cluttered environments. Simulation results showed that the manifold-based approach achieved improved communication performance with lower computational complexity and faster convergence compared with conventional (Semidefinite Programming) SDP-based optimization methods. Zhang and Cao [13] proposed an active RIS-assisted ISAC system to jointly enhance communication and sensing performance. The study considered a joint beamforming design for both the BS and the active RIS by employing a deep reinforcement learning-based approach to address the high complexity of the non-convex optimization formulation in RIS-enabled ISAC systems. The results demonstrated that the use of active RIS can effectively improve system efficiency and achieve better sum-rate and sensing performance compared with conventional methods. Wang et al. [14] introduce a design of a target localization system using an RIS-assisted passive radar system for ISAC in a 6G system. They utilize particular algorithms to estimate the number of targets along with the target locations based on angle of arrival and time of arrival. While Liu et al. [15] investigate an RIS-assisted MU-multiple-input single-output (MISO) ISAC system with joint beamforming and reflection optimization under SNR and Cram´er-Rao bound (CRB) based sensing constraints. Efficient algorithms are developed to maximize communication sum-rate while ensuring detection and estimation performance, and simulations confirm notable sensing and communication gains with larger RIS arrays. In reference [16], fractional programming (FP) algorithm was leveraged to optimize the BS transmit beamforming and RIS phase shifts for the RIS-enabled ISAC system with the objective of maximizing the sum-rate.

Recent studies have increasingly investigated RIS-assisted ISAC systems for 6G networks, focusing mainly on joint active beamforming at the BS and passive beamforming at the RIS. Most existing works formulate the problem as a non-convex optimization problem and solve it using FP, majorization-minimization, penalty-based methods, or semidefinite relaxation. Although these methods can achieve promising performance, their computational complexity may increase significantly with the number of RIS reflective elements and active users. In addition, many existing studies mainly emphasize achievable sum-rate or sensing SNR separately, while the joint impact of RIS optimization on sum-rate, outage probability, and sensing sum-SNR is less explicitly discussed. Therefore, this work aims to address this limitation by employing a Weighted minimum mean square error (WMMSE)-based beamforming framework integrated with manifold optimization for RIS phase shifts, while evaluating both communication reliability and sensing performance. This paper investigates the beamforming strategies of an RIS-aided ISAC system, in which a multi-antenna BS simultaneously provides communication services to multiple single-antenna user equipment (UEs) and performs target sensing.

The objective is to jointly optimize the beamforming matrix and reflection coefficient profile matrix to improve both the communication sum-rate and sensing sum-SNR while satisfying the communication QoS and other communication constraints. WMMSE-based optimization approach is employed to efficiently design the transmit beamformers at the BS under a certain power constraint. Meanwhile, the RIS reflection coefficients under unit-modulus requirements are optimized via manifold optimization techniques. Considering constraints on the beamforming matrix and the phase shifts of the RIS elements, an alternating optimization approach is employed to alternately update the optimization variables.

The key contributions of this study are presented below:

- A joint beamforming framework is introduced for RIS-assisted MU-MISO ISAC systems, where the BS beamforming and RIS phase shifts are optimized together.
- WMMSE is used to optimize the transmit beamforming at the BS for sum-rate improvement under the transmit power constraint.
- The RIS phase shifts are optimized using manifold optimization while maintaining the unit-modulus constraint.
- The proposed system is assessed in key metrics of achievable sum-rate, outage probability, and sensing sum-SNR.
- Furthermore, utilizing WMMSE instead of conventional approaches, such as the FP method in reference [16], reduces computational complexity, as highlighted in references [17, 18].
- The simulation results confirm the performance improvement of the proposed RIS-assisted ISAC system compared with random RIS and without RIS cases.

This paper is organized as follows. Section 1 introduces the background and motivation of the study. Section 2 describes the system model. Section 3 presents the proposed algorithm and its analysis. Section 4 discusses the simulation model and results. Finally, Section 5 concludes the paper.

2. SYSTEM MODEL

The considered multiple-user MISO downlink ISAC system consist of a BS employing M antennas serves K single-antenna UEs with the assistant of RIS has N elements, while performing sensing operations for T targets. In particular, the RIS is placed close to the served users to enable effective support for downlink multi-user communication, where the targets locations are far away from the RIS and have a strong direct line-of-sight (LoS) path with the BS, the sensing echo signals observed by the RIS are weak and can be ignored, as assumed in reference [19]. This deployment scenario is adopted to follow commonly used RIS-assisted ISAC models, where the RIS mainly enhances the communication links while the BS-target LoS path dominates the sensing process. Although the considered setup assumes a LoS-dominant environment, more challenging propagation conditions such as NLoS transmission, shadowing effects, and interference-rich environments may influence the overall system performance. These scenarios are considered important future research directions for RIS-assisted ISAC systems. The considered system is shown in Figure 1.

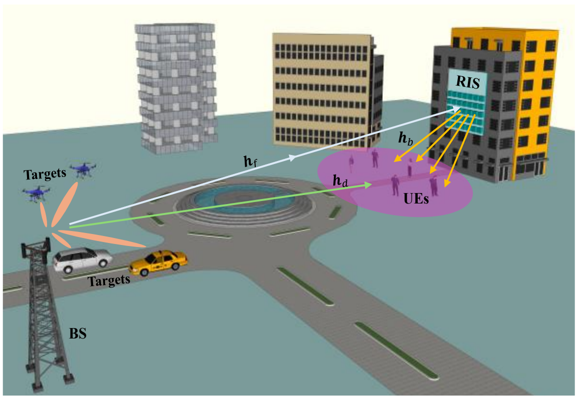

Figure 1. The reconfigurable intelligent surfaces (RIS)-enabled integrated sensing-and-communications (ISAC) model

The transmit signal at the BS can be given by [11, 20],

$$x = F_c s_c + F_s s_s = Fs \tag{1}$$

where, $F_C \in \mathbb{C}^{M\times K}$ denotes the communication beamforming matrix, $F_s \in \mathbb{C}^{M\times M}$ represent the sensing beamforming matrix. The $s_c \in \mathbb{C}^K$ and $s_s \in \mathbb{C}^M$ represent the communication symbol vector with $\mathbb{E}\{s_c s_c^H\} = I_K$ and the sensing signal with $\mathbb{E}\{s_s s_s^H\} = I_M$, respectively, and they are assumed to be statistically uncorrelated. Specifically, the complete beamforming matrix is represented by $F \triangleq [F_c F_s] \in \mathbb{C}^{M\times(K+M)}$ and the transmit symbol vector can be written as $s \triangleq [s_c^T s_s^T]^T \in \mathbb{C}^{(K+M)}$ [11, 20].

The received signal at the UE is delivered through two propagation paths: the direct LoS link and the RIS-reflected virtual line-of-sight (VLoS) link, which is the RIS-assisted reflected link. Then, the channel model will consist of the direct path channel $h_d \in \mathbb{C}^M$, from the BS to and the UE, and the cascaded path channel h_{VLoS}, from BS to RIS then to UE, which consist of forward channel $h_f \in \mathbb{C}^{N\times M}$ extending from the BS toward the RIS and backward channel $h_b \in \mathbb{C}^N$ from the RIS toward the UE include the RIS reflection effects and can be written as [21, 22].

$$h_{VLoS} = h_b^T \Phi h_f \tag{2}$$

where, the effect of RIS on the incident signal can be described by a diagonal matrix associated with the RIS phase coefficients $\varphi \triangleq [\varphi_1, \dots, \varphi_N]^T$ with $|\varphi_n|, \forall_n$, *i.e.*, $\Phi \triangleq diag(\varphi)$. Consequently, the received signal corresponding to the k^{th} user can be formulated as [11]:

$$y_k = (h_{d,k} + h_{VLoS,k})x + n_k \tag{3}$$

The scalar $n_k \sim \mathcal{CN}(0, \sigma_k^2)$ denotes an additive noise that is modeled as a complex Gaussian random variable with variance of σ^2. Accordingly, the signal to interference plus noise ratio (SINR) experienced by the k^{th} is given by:

$$\gamma_k = \frac{|(h_{d,k} + h_{VLoS,k})f_k|^2}{\sum_{j=1, j\neq k}^{K+M} |(h_{d,k} + h_{VLoS,k})f_j|^2 + \sigma_k^2} \tag{4}$$

where, f_j represents the j^{th} column vector of the beamforming matrix F for $j = 1, \dots, K+M$. Therefore, the aggregate sum-rate achieved by all users can be expressed [16]:

$$R = \sum_{k=1}^{K} log_2(1 + \gamma_k) \tag{5}$$

From a sensing standpoint, to achieve superior sensing performance, maximizing signal power is a common adopted objective as in reference [11, 23]. Then, the sensing SNR_s is given as [11]:

$$SNR_s = \frac{\eta_{echo} h_{BT}^T F F^H h_{BT}}{\sigma^2} \tag{6}$$

where, h_{BT} denotes the channel between BS and the target, η_{echo} corresponds to the target reflection coefficient, while σ^2 denotes the noise power. The sensing SNR expression is derived from the standard radar signal model, where the received power is modeled as $h_{BT}^T F F^H h_{BT}$, and then normalized by the noise power [23].

The matrices of the beamforming and the RIS reflection coefficient, F and ϕ, respectively, are optimized in a coupled manner to maximize the achievable communication sum-rate, subject to the communication QoS constraints and the transmit power limitation. The corresponding optimization problem is formulated as,

$$\max_{F,\Phi} \sum_{k=1}^{K} log_2(1 + \gamma_k) \tag{7a}$$

$$\text{s.t.} \sum_{t=1}^{T} \frac{\eta_{echo} \boldsymbol{h}_{BT}^T F F^H \boldsymbol{h}_{BT}}{\sigma_s^2} \geq \Gamma_s, \tag{7b}$$

$$||F||_F^2 \leq P \tag{7c}$$

$$|\varphi_n| = 1, \forall_{n,} \tag{7d}$$

where, P denotes the available transmit power and Γ_s represents the sensing SNR threshold. The problem in Eq. (7) poses significant challenges and difficulties to optimize. That is a result of the non-convex objective function in Eq. (7a) and the additional sensing and unit-modulus constraints in Eq. (7b) and Eq. (7d), respectively. Accordingly, the WMMSE framework is adopted to handle the objective function in Eq. (7a). The original optimization problem is then divided into two tractable subproblems, which are solved through iterative optimization procedures. The communication QoS can be represented by outage probability. The outage probability is defined as a reliability metric for the considered system. An outage event occurs when the achievable rate falls below a predefined threshold due to channel variations, which is a widely adopted definition in wireless communication systems [24, 25]. Then, based on the achievable sum-rate expression in Eq. (5).

$$P_{out} = P_r\left(R_{bps} < R_{th}\right) \tag{8}$$

where, R_{th} denotes the minimum required data rate. Since the system bandwidth is fixed to B, the achievable throughput in bits per second (bps) is obtained as:

$$R_{bps} = B \times R = B \sum_{k=1}^{K} log_2(1+\gamma_k) \tag{9}$$

Accordingly, an outage event is declared whenever the achievable throughput cannot satisfy the target rate requirement.

3. PROPOSED ALGORITHM

This section presents a structured algorithm that is proposed to be used for solving the non-convex sum-rate maximization problem. A WMMSE framework is adopted to reformulate the original objective function into an equivalent weighted mean square error optimization problem for designing the transmit beamforming matrix at the BS. Owing to the different natures and constraints of the transmit beamforming variables and the RIS phase-shift variables, the overall optimization problem is decomposed into two separate subproblems. Specifically, the transmit beamformers are optimized using the WMMSE approach under the available transmit power limit, while the RIS phase vector is optimized under the unit-modulus constraint. The interaction between these two subproblems is implicitly captured through the effective channel, and the overall solution is obtained via an alternating optimization. In the proposed alternating optimization framework, the transmit beamforming matrix is first updated using the WMMSE approach for fixed RIS phase shifts. Then, the RIS phase vector is optimized using manifold optimization while keeping the beamforming matrix fixed. This iterative process continues until convergence or until the maximum number of iterations is reached. The RIS phase vector is initially generated with random phases satisfying the unit-modulus constraint.

3.1 Weighted minimum mean square error-based beamforming optimization

The WMMSE algorithm solves the sum-rate maximization problem by equivalently minimizing the weighted MSE. It alternates between updating the receiver filter, the MSE weight, and the transmit beamformer, where each subproblem admits a closed-form solution. The beamformer for the k^{th}, which is the solution of the WMMSE, is computed as [18].

$$\bar{B}_k = \left(\sum_{i=1}^{K} H_i A_i^H W_i A_i H_i^H + \frac{\sum_{i=1}^{K} Tr\left(A_i^H W_i A_i\right)}{E_{tx}/_{\sigma^2}} I_M\right)^{-1} \times H_k A_k^H W_k \tag{10}$$

In Eq. (10), $H_i \in \mathbb{C}^{M\times 1}$ denotes the channel vector between the BS and the i^{th} user, while H_k corresponds to the channel vector of the target user for which the transmit beamformer is being updated, the matrix $A_i \in \mathbb{C}^{1\times 1}$ denotes the MMSE receiver coefficient of the i^{th} user, and W_i represents the corresponding MSE weight in the WMMSE framework. The operator (Tr) denotes the trace of a matrix, defined as the sum of its diagonal elements, E_{tx} denotes the total transmit power constraint at the BS, while σ^2 represents the noise variance, and the matrix I_M denotes the $M \times M$ identity matrix.

In Eq. (10), for the considered single-antenna users, the MMSE receiver coefficient for user A_k and the MSE weight W_k reduce to scalar values given as in reference [17]:

$$A_k = B_k^H H_k \left(\sum_{i=1}^{K} H_k^H B_i B_i^H H_k + \sigma^2\right)^{-1} \tag{11}$$

$$W_k = 1 + B_k^H H_k B_{\overline{nk}}^{-1} H_k^H B_k \tag{12}$$

For the considered single-antenna UEs case, the index i represents a generic user and is employed in the summation to model the interference from all users. In each WMMSE update step, the MMSE receiver coefficient A_k and the corresponding weighting factor W_k first evaluated for all k, subsequently the power normalization factor is given by $b = \sqrt{E_{tx}/Tr(\bar{B}\bar{B}^H)}$, where $\bar{B} = [\bar{B}_1 \cdots\cdots \bar{B}_k]$, E_{tx} is the total transmit power, and the WMMSE beamformer becomes:

$$B_k^{WMMSE} = b\bar{B}_k \tag{13}$$

The following algorithm illustrates the steps of the proposed procedure.

Algorithm 1. WMMSE-based beamforming optimization

Input: Channel vectors H_k, noise power σ^2, total transmit power E_{tx}

Objective: Obtain the transmit beamforming solution B_k for sum-rate enhancement.

Initialize: The transmit beamformers B_k for all users k = 1,…,K

Repeat

1: Update the MMSE receiver filter A_k using Eq. (11)

2: Update the MSE weight matrix W_k using Eq. (12)

3: Update the transmit beamformer B_k using Eq. (10)

4: Normalize the beamformers to satisfy the power constraint using Eq. (13)

5: Convergence or maximum number of iterations is reached? If not, go to repeat.

End

Output: Optimized transmit beamformers B_k for all users

3.2 Manifold-based optimization of reconfigurable intelligent surface phase shifts

In this subsection, the RIS phase shift vector φ is jointly optimized together with transmit beamformers. Owing to the passive nature of the RIS, each element is subject to a unit-modulus constraint $|\varphi_n| = 1$. The resulting optimization problem is reformulated into an equivalent quadratic form, enabling an efficient solution via manifold optimization techniques. The optimization problem with respect to the RIS phase shifts ϕ is given as [26]:

$$\max_{\phi} \sum_{k=1}^{K} \left(2\sqrt{1+c_k}\,\Re\{g_k^* h_k^H f_k\} - |g_k|^2 \sum_{j=1}^{K+M} \left|h_k^H f_j\right|^2\right) \quad (14)$$

$$s.t.\, |\varphi_n| = 1, \forall_n \quad (15)$$

Then $h_{VLoS} = h_b^T \Phi h_f f_j = h_b^T diag(h_f f_j)\phi$, problem re-arranged as:

$$\min_{\phi} \phi^H Q \phi - 2\Re\{\phi^H q\} - c \quad (16)$$

$$s.t.\, |\varphi_n| = 1, \forall_n \quad (17)$$

$$Q \triangleq \sum_{k=1}^{K} |g_k|^2 \sum_{j=1}^{K+M} \mathrm{diag}(f_j^H h_f{}^H) h_b\, h_b^T \mathrm{diag}(h_f f_j) \quad (18)$$

$$q \triangleq \sum_{k=1}^{K} \sqrt{1+c_k}\, g_k \mathrm{diag}(f_k^H h_f{}^H) h_b - \sum_{k=1}^{K} |g_k|^2 \sum_{j=1}^{K+M} \mathrm{diag}(f_j^H h_f{}^H) h_b\, h_b^T f_j^H \quad (19)$$

$$c = \Re\left\{\sum_{k=1}^{K} 2\sqrt{1+c_k}\, g_k^* \mathrm{h}_{d,k}^H f_k - |g_k|^2 \sum_{j=1}^{K+M} |\mathrm{h}_{d,k}^H f_j|^2\right\} \quad (20)$$

The auxiliary variable g_k represents the MMSE receiver coefficient [16], while c_k denotes the SINR-related parameter associated with user k. Furthermore, $Q \in \mathbb{C}^{N\times N}$ is a Hermitian matrix that characterizes the overall interference structure arising in the quadratic reformulation of the problem and $q \in \mathbb{C}^{N\times 1}$ corresponds to the linear component linked to the desired signal term.

The scalar c is a constant independent of the RIS phase vector φ and, therefore, does not influence the optimization outcome. Algorithm 2 illustrates the steps of the proposed procedure.

Algorithm 2. Manifold-based optimization of RIS phase shifts

Input: $h_f, h_b, h_{d,k}, f_j, g_k, c_k, M, I_{max}$

Objective: Optimize ϕ by solving Eq. (16)

Initialize: RIS phase vector φ such that $|\varphi_n| = 1$

Repeat

1: Compute Q using Eq. (18)

2: Compute q using Eq. (19)

3: Compute c using Eq. (20)

4: Update ϕ by solving the equivalent manifold using Eq. (16)

5: Retract/normalize $\varphi \leftarrow e^{j\varphi_n}$ to satisfy $|\varphi_n| = 1$ Eq. (15)

6: Convergence or maximum number of iterations I_{max} is reached? If not, go to repeat.

End

Output: Optimized RIS phase-shift vector φ

3.3 Computational complexity analysis

The computational complexity of the proposed framework is incurred during the WMMSE beamforming and the manifold-based refinement of the RIS reflection coefficient optimizations. In the WMMSE stage, the dominant computational operation is the inversion of an $M \times M$ matrix, resulting in a complexity order approximately proportional to $O(M^3)$. In addition, the iterative updates of the receiver coefficients and MSE weights introduce additional complexity proportional to the number of users *K*. In the RIS optimization step, the required computational effort is primarily influenced by the number of RIS elements *N*, since the construction of the quadratic matrices and manifold gradient updates involve operations on *N*-dimensional vectors and matrices. Therefore, the computational burden increases as the RIS size becomes larger. Moreover, the overall computational cost of the proposed method is affected by the number of alternating optimization iterations required for convergence. Although larger RIS configurations can provide higher passive beamforming gains, they also increase the optimization complexity. Nevertheless, compared with conventional FP-based optimization approaches, the adopted WMMSE framework provides a more structured iterative optimization process with practical computational scalability for RIS-assisted MU-MISO ISAC systems.

4. SIMULATION MODEL AND RESULTS

The performance of the proposed joint beamforming design and phase shift profile for the RIS-assisted ISAC *system* is numerically evaluated in this section. The considered system has BS integrated with $M = 8$ antennas with half-wavelength spacing. Also, $K = 4$ single-antenna users are served with the assistance of an RIS consisting of $N = 169$ elements. In addition, a noise of power $\sigma_u^2 = -80$ dBm is considered. Furthermore, the distances of BS-RIS is set as $50\ m$, nd RIS-UE is set as $4\ m$. A distance-dependent path-loss model is modeled, where the path-loss exponents are set to $\alpha_{Bu} = 3.5$, $\alpha_{Br} = 2.5$ and $\alpha_{Ru} = 2.5$ for the BS-UE, BS-RIS, and RIS-UE links, respectively. In terms of the channel model, the channel is assumed to be subject to Rician fading with Rician factor $\beta_{Ru} = 3$ dB and $\beta_{Bu} = 0$, The considered values are consistent with the suggested literature such as in reference [16, 27].

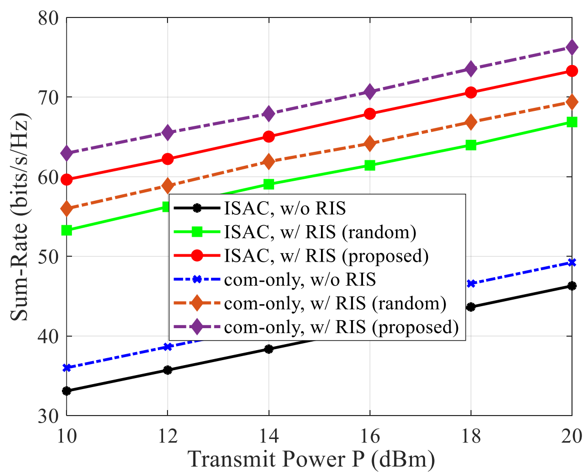

Figure 2. Sum-rate vs transmit power (dBm)

Figure 2 presents the sum-rate plotted versus the transmit power for both ISAC and communication systems under different RIS deployment strategies. It can be observed that the sum-rate consistently increases with transmit power across all configurations. From all these systems, the optimized RIS configuration attains the highest performance, outperforming both the random RIS and without RIS scenarios. Furthermore, the communication only system achieves higher sum-rate values than the ISAC system, since ISAC jointly allocates its available resources to sensing and communication functionalities. In communication only system, the sum-rate reached 49 bps/Hz without RIS. However, by integrating the proposed RIS, the performance significantly increased to 76 bps/Hz, achieving a remarkable improvement rate of 55%.

Figure 3 illustrates the impact of varying the number of RIS elements on the sum-rate for both the ISAC system and the communication only system. A comparison between random and optimized phase shifts strategies, in addition to without RIS case. It can be observed that increment in the number of RIS elements leads to a higher sum-rate for both random and optimized RIS phase configurations, which can be attributed to the array gains and the effectiveness of passive beamforming for increasing the equivalent channel and signal power received. As the number of RIS elements increases, the sum-rate continues to improve for both ISAC and communication-only systems. However, the improvement becomes smaller at large values of N. It is due to the reason this behavior can be attributed to the limited transmit power budget and the residual multi-user interference. In the ISAC framework, a portion of the available transmit power is allocated to sensing operations, which reduces the amount of power available for communication compared with the communication-only system. Additionally, it is clear that the performance of the phase optimization configuration is better compared to the random phase shift configuration for all values of N. However, the communication-only system is higher compared to the sum-rate achievable for the ISAC system for all values of N. This is expected since in the conventional system, the entire power is used for the communication signal, while in the ISAC system, the power is divided between the communication and sensing signals.

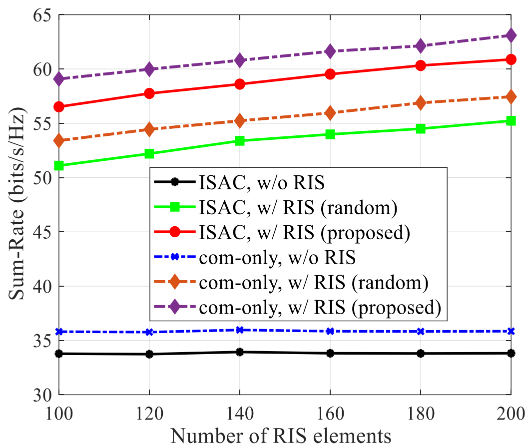

Figure 3. Sum-rate vs numbers of reconfigurable intelligent surfaces (RIS) elements

Figure 4 illustrates the effect of the number of BS antennas M on the achievable sum-rate for the ISAC and the communication only system. It is observed that the achievable sum-rate improves as the number of BS antennas M increases. Among all configurations, the optimized RIS, followed by the random RIS configuration compared with no RIS case.

Figure 5 presents the impact of varying the number of users K on the achievable sum-rate in both ISAC and communication-only systems. The sum-rate increases with K in all cases due to multi-user diversity. The optimized RIS configuration achieves the highest performance, followed by the random RIS case compared with the case without RIS. Moreover, the communication only system consistently outperforms the ISAC system since ISAC shares its resources between sensing and communication. In this work, all users are assumed to have similar communication requirements. Future studies may consider users with different QoS demands in order to further evaluate the performance of RIS-assisted ISAC systems under heterogeneous user conditions.

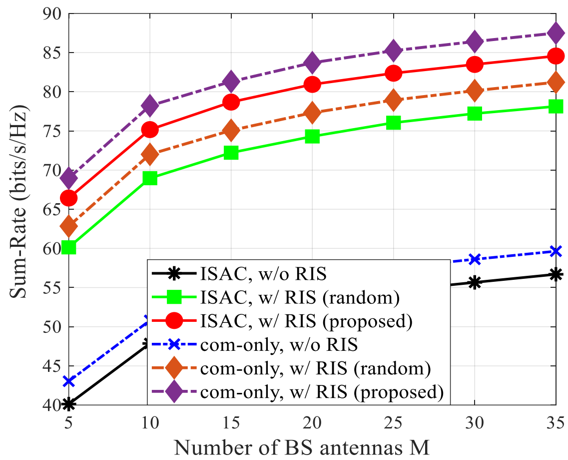

Figure 4. Sum-rate vs numbers of base station (BS) antennas

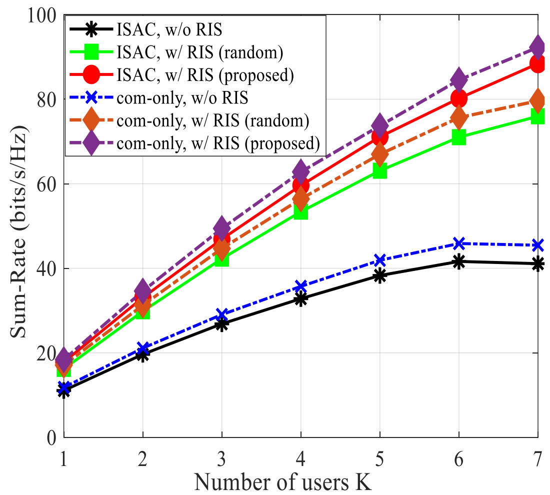

Figure 5. Sum-rate vs numbers of users

Outage probability versus SNR for different numbers of RIS elements under the proposed RIS phase is analyzed and the results are depicted in Figures 6 and 7. Figure 6 shows the outage probability for ISAC, while Figure 6 presents the outage probability for communication only scenario. A noticeable reduction in outage probability is achieved with increasing SNR across all considered values of N, indicating improved communication reliability in both ISAC and communication only cases. Due to the power consumption for sensing in the ISAC case, a part of the available transmit power is reserved for sensing operations, reducing the power resources available for data transmission. Furthermore, increasing the number of RIS elements results in a clear reduction in outage probability. This improvement can be explained by the enhancement of the effective channel gain due to the increased array gain provided by a larger RIS.

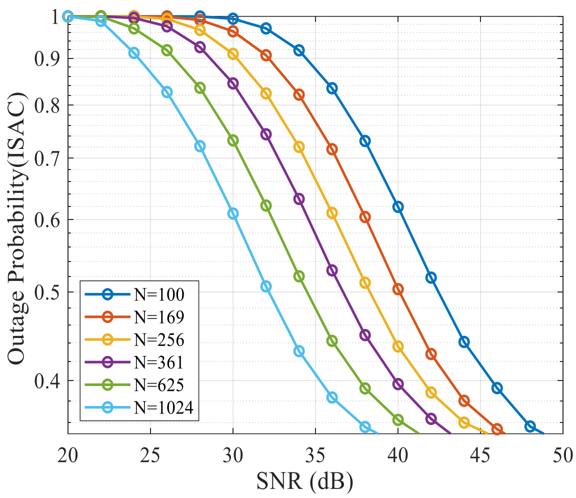

Figure 6. Outage probability vs SNR for ISAC
Note: signal-to-noise ratio (SNR); integrated sensing-and-communications (ISAC)

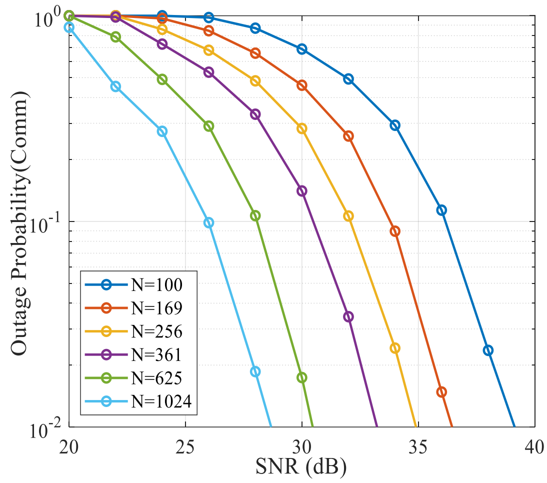

Figure 7. Outage probability vs SNR for communication
Note: signal-to-noise ratio (SNR)

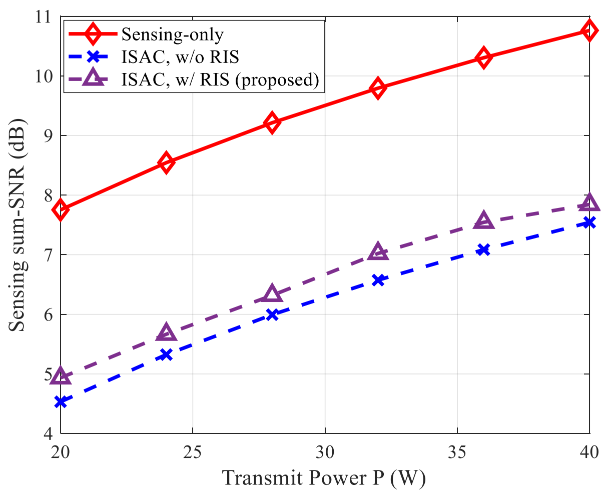

Figure 8. Sensing sum-SNR (dB) vs transmit power

Figure 8 shows the sensing sum-SNR at BS versus the transmit power for both sensing-only and ISAC systems. It can be observed that the sensing-only scheme achieves the highest SNR since all transmit power is dedicated to target sensing. By incorporating RIS, the proposed ISAC scheme achieves a noticeable improvement in sensing SNR, which enhances the capability of the system to detect the target more reliably, while without RIS shows reduced sensing performance. This improvement is attributed to the enhanced effective channel. In this work, the sensing performance is evaluated using the sensing sum-SNR metric. Other sensing metrics, such as target detection accuracy and localization performance, are not considered and may be investigated in future studies.

5. CONCLUSIONS

The performance of an RIS-assisted ISAC system is studied in this paper, with particular emphasis on sum-rate enhancement and reliability improvement in addition to the sensing sum-SNR. The WMMSE optimization approach is used to obtain the transmit beamforming at BS, while a manifold-based approach is used to optimize the RIS phase shift profile under certain constraints. From the simulation results, it is found that the proposed RIS-assisted ISAC design achieves superior performance compared to both the system without RIS and the randomly configured RIS case, in terms of sum-rate. Furthermore, outage probability is considered as a reliability-metric to assess the performance of the proposed ISAC framework. Also, sensing sum-SNR is considered, and comparison between the communication-only system and the ISAC system is evaluated. An intrinsic trade-off between communication efficiency and sensing performance exists, thus forming a fundamental property of ISAC systems. So, the proposed approach can be considered as a good solution to ISAC systems with the help of an RIS, thus forming a foundation for future research in this direction. In practical systems, the performance of RIS-assisted ISAC may also be affected by hardware limitations, imperfect channel estimation, and phase noise. Although additive noise is considered in the system model, other practical impairments were not investigated in this work and may affect the overall system performance in real deployment scenarios. Future work can study the use of more than one RIS in the ISAC system. In this case, better performance may be achieved, but the optimization and system design will become more difficult. Dynamic RIS adaptation can also be considered in future studies.

REFERENCES

[1] Liu, F., Cui, Y.H., Masouros, C., Xu, J., Han, T.X., Eldar, Y.C. (2022). Integrated sensing and communications: Toward dual-functional wireless networks for 6G and beyond. IEEE Journal on Selected Areas in Communications, 40(6): 1728-1767. https://doi.org/10.1109/JSAC.2022.3156632

[2] Kaushik, A., Singh, R., Dayarathna, S., Senanayake, R., Di Renzo, M., Dajer, M. (2024). Toward integrated sensing and communications for 6G: Key enabling technologies, standardization, and challenges. IEEE Communications Standards Magazine, 8(2): 52-59. https://doi.org/10.1109/MCOMSTD.0007.2300043

[3] Alhafid, A.K., Mohammed Ali, Y.E., Younis, S. (2024). Far-field localization for RIS empowered wireless systems leveraging beamforming. Jordan Journal of Electrical Engineering, 10(3): 484-499. https://doi.org/10.5455/jjee.204-1701118386

[4] Alhafid, A.K., Ali, Y.E.M., Younis, S. (2023). Performance investigation of RIS aided localization with TDoA in the near-field. Mathematical Modelling of Engineering Problems, 10(6): 2127-2134. https://doi.org/10.18280/mmep.100624

[5] Alghannam, A.I., Alhafid, A.K. (2020). Performance analysis of unsolicited grant service (UGS) service class in WiMAX voip application. Journal of Engineering Science and Technology, 15(3): 1481-1491.

[6] Chopra, G., Ahmed, S. (2025). Ris-assisted integrated sensing and communication: Applications, challenges and usecase scenario. Discover Applied Sciences, 7(7): 650. https://doi.org/10.1007/s42452-025-07098-8

[7] Haider, M.A., Zhang, Y.D. (2023). RIS-aided integrated sensing and communication: A mini-review. Frontiers in Signal Processing, 3: 1197240. https://doi.org/10.3389/frsip.2023.1197240

[8] Zhang, D., Cui, Y.H., Cao, X.W., Su, N.C., Gong, Y., Liu, F. (2026). Integrated sensing and communications over the years: An evolution perspective. IEEE Communications Surveys & Tutorials, 28: 5014-5048. https://doi.org/10.1109/COMST.2026.3655674

[9] Liu, G.Y., Han, L.C., Xi, R.Y., Ma, L., Han, Z.X., Xue, Y.H., Zhao, H.T., Jin, J., Wang, Q.X., Xu, F. (2025). Cooperative sensing for 6G ISAC: Concept, key technologies, performance evaluation, and field trial. Engineering, 56: 130-148. https://doi.org/10.1016/j.eng.2025.08.033

[10] Sheet, Y.S., Alsharbaty, F.S., Thanoun, M.Y. (2025). Optimizing wireless networks for automated guided vehicles and remote-control systems in smart factory. In 2025 International Conference on New Trends in Computing Sciences (ICTCS), Amman, Jordan, pp. 20-25. https://doi.org/10.1109/ICTCS65341.2025.10989477

[11] Luo, H.H., Liu, R., Li, M., Liu, Q. (2023). RIS-aided integrated sensing and communication: Joint beamforming and reflection design. IEEE Transactions on Vehicular Technology, 72(7): 9626-9630. https://doi.org/10.1109/TVT.2023.3248657

[12] Samir, A., Ibrahim, A.S., Ismail, M.H., Elsayed, M. (2026). Sum rate optimization via joint beamforming in RIS-assisted ISAC system: A manifold-based approach. IEEE Open Journal of the Communications Society, 7: 786-801. https://doi.org/10.1109/OJCOMS.2025.3649379

[13] Zhang, W.H., Cao, K.T. (2026). Beamforming design for active RIS-aided ISAC systems: A deep reinforcement learning approach. IEEE Communications Letters, 30: 105-109. https://doi.org/10.1109/LCOMM.2025.3632148

[14] Wang, D., Bazzi, A., Chafii, M. (2024). RIS-enabled integrated sensing and communication for 6G systems. In 2024 IEEE Wireless Communications and Networking Conference (WCNC), Dubai, United Arab Emirates, pp. 1-6. https://doi.org/10.1109/WCNC57260.2024.10571090

[15] Liu, R., Li, M., Liu, Q., Swindlehurst, A.L. (2024). SNR/CRB-constrained joint beamforming and reflection designs for RIS-ISAC systems. IEEE Transactions on Wireless Communications, 23(7): 7456-7470. https://doi.org/10.1109/TWC.2023.3341429

[16] Luo, H.H., Liu, R., Li, M., Liu, Y., Liu, Q. (2022). Joint beamforming design for RIS-assisted integrated sensing and communication systems. IEEE Transactions on Vehicular Technology, 71(12): 13393-13397. https://doi.org/10.1109/TVT.2022.3197448

[17] Choi, H., Swindlehurst, A.L., Choi, J. (2024). WMMSE-based rate maximization for RIS-assisted MU-MIMO systems. IEEE Transactions on Communications, 72(8): 5194-5208. https://doi.org/10.1109/TCOMM.2024.3381707

[18] Shen, K.M., Yu, W. (2018). Fractional programming for communication systems-part I: power control and beamforming. IEEE Transactions on Signal Processing, 66(10): 2616-2630. https://doi.org/10.1109/TSP.2018.2812733

[19] Wang, X.Y., Fei, Z.S., Zheng, Z., Guo, J. (2021). Joint waveform design and passive beamforming for RIS-assisted dual-functional radar-communication system. IEEE Transactions on Vehicular Technology, 70(5): 5131-5136. https://doi.org/10.1109/TVT.2021.3075497

[20] Liu, X., Huang, T.Y., Shlezinger, N., Liu, Y.M., Zhou, J., Eldar, Y.C. (2020). Joint transmit beamforming for multiuser MIMO communications and MIMO radar. IEEE Transactions on Signal Processing, 68: 3929-3944. https://doi.org/10.1109/TSP.2020.3004739

[21] Alhafid, A.K., Younis, S., Mohammed Ali, Y.E. (2024). Efficient near-field localization aided with reconfigurable intelligent surface using geometric dilution of precision. Journal of Information and Telecommunication, 8(2): 208-230. https://doi.org/10.1080/24751839.2023.2272488

[22] Alhafid, A.K., Younis, S., Ali, Y.E.M. (2024). Enhanced far-field localization scheme using multi-RIS and efficient beam sweeping. Progress In Electromagnetics Research C, 140: 163-175. https://doi.org/10.2528/PIERC23112903

[23] Li, J., Stoica, P. (2007). MIMO radar with colocated antennas. IEEE Signal Processing Magazine, 24(5): 106-114. https://doi.org/10.1109/MSP.2007.904812

[24] Parihar, A.S., Singh, K., Bhatia, V., Shin, H., Niyato, D. (2026). On the outage and sensing performance of multi-sector RIS-assisted ISAC networks. Technology Research Archive, pp. 1-15. https://doi.org/10.36227/techrxiv.177083705.59954340/v1

[25] Wang, T.X., Badiu, M.A., Chen, G.J., Coon, J.P. (2021). Outage probability analysis of RIS-assisted wireless networks with von Mises phase errors. IEEE Wireless Communications Letters, 13(12): 2737-2741. https://doi.org/10.1109/LWC.2021.3113830

[26] De Souza Junior, W., Guerra, D.W.M., Filho, J.C.M., Abrao, T., Hossain, E. (2024). Manifold-based optimizations for RIS-aided massive MIMO systems. IEEE Open Journal of the Communications Society, 5: 7913-7940. https://doi.org/10.1109/OJCOMS.2024.3512662

[27] Wu, Q.Q., Zhang, R. (2019). Intelligent reflecting surface enhanced wireless network via joint active and passive beamforming. IEEE Transactions on Wireless Communications, 18(11): 5394-5409. https://doi.org/10.1109/TWC.2019.2936025

NOMENCLATURE

s	transmit symbol vector
s_c	communication symbol vector
s_s	sensing symbol vector
h_d	direct path channel
h_f	forward channel
h_b	backward channel
h_{vLos}	cascaded channel
y_k	observed signal at the k^{th} user
h_{BT}	channel between BS and the target
γ_k	SINR
R	sum rate
σ^2	additive noise power
P_{out}	outage probability
B	bandwidth
R_{bps}	achievable throughput in bits per second
R_{th}	minimum required data rate
P	transmit power
A_k	MMSE receiver filter
W_k	update the MSE weight matrix
B_k	transmit beamformer
g_k	MMSE receiver coefficient
c_k	SINR-related parameter associated with user k
Q	Hermitian matrix
q	linear component linked to the desired signal term

Greek symbols

Φ	RIS phase matrix
η_{echo}	target reflection coefficient
Γ_s	sensing SNR threshold
i	i-th user
α	path-loss
β	Rician factor